An Experimental Investigation of Directly Injected E85 Fuel in a Heavy-Duty Compression Ignition Engine

Novakovic, Maja; Tunér, Martin; Garcia, Antonio; Verhelst, Sebastian

Published in:
SAE Powertrains, Fuels & Lubricants Conference & Exhibition

DOI:
10.4271/2022-01-1050

2022

Document Version:
Peer reviewed version (aka post-print)

22FFL-0198

An Experimental Investigation of Directly Injected E85 Fuel in a Heavy-Duty Compression Ignition Engine

Maja Novakovic[a], Martin Tuner[a], Antonio Garcia[b], Sebastian Verhelst[a, c]
[a]Lund University
[b] Universitat Politecnica de Valencia
[c]Ghent University

Abstract

A commercially available fuel, E85, a blend of ~85% ethanol and ~15% gasoline, can be a viable substitute for fossil fuels in internal combustion engines in order to achieve a reduction of the greenhouse gas (GHG) emissions. Ethanol is traditionally made of biomass, which makes it a part of the food-feed-fuel competition. New processes that reuse waste products from other industries have recently been developed, making ethanol a renewable and sustainable second-generation fuel. So far, work on E85 has focused on spark ignition (SI) concepts due to high octane rating of this fuel. There is very little research on its application in CI engines. Alcohols are known for low soot particle emissions, which gives them an advantage in the NOx–soot trade-off of the compression ignition (CI) concept. Therefore, the main objective of this research is to experimentally characterise the impact of E85 on performance and emissions of a heavy-duty (HD) direct ignition compression ignition (DICI) engine at mid-to-low load, and to identify possible challenges. To do so, a surface response method of the Box-Behnken type is implemented on a measurement campaign on a HD single cylinder CI engine. The effects of common rail pressure (P_{rail}), λ and combustion timing (CA50) as control parameters on experimentally measured values of soot, regulated gaseous emissions (NOx, CO and THC) and gross indicated efficiency (GIE) of the engine are studied. Linear regression (LR) analysis indicates that the outputs of the NOx and soot models are affected by all three control parameters, whereas GIE, THC and CO models in this case exclude λ effects. E85 fuel shows potential to be a good candidate for highly efficient low temperature combustion (LTC) in DICI engines, with reduced NOx and soot levels compared to fossil diesel combustion.

Introduction

Long-term improvements and plans for solving challenges in transportation until year 2050 have been in focus of governments and policy makers world-wide. While trying to change our consumption and travelling habits and waiting for new discoveries to emerge, we have an obligation to improve the current state of the technology in such a way that the global warming and pollution from the internal combustion engines (ICEs) be reduced. A small increase in engine efficiency, a slight reduction of harmful emissions, and blending higher percentages of renewable fuels into fossil ones, can add up to a significant improvement. In order to achieve the reduction of the greenhouse gas (GHG) emissions, The European Union promotes the use of energy from renewable sources. [1].

Direct injection compression ignition (DICI) diesel engines are renowned for their high efficiency, durability and high torque output, and therefore are an element of the transportation that can keep its place in the changing technology. By combusting E85 instead of fossil-based diesel, DICI engines can reduce their climate impact. The challenge is to ignite E85 in a DICI engine due to its high research octane number (RON) and low cetane number (CN), which can be solved by emerging technologies [2][3].

E85 is a fuel consisting of up to 85% anhydrous ethanol by volume mixed with gasoline without aromatics; the composition is 85% ethanol and 15% gasoline during the summer time, and 75% ethanol and 25% gasoline during the winter time. It is commonly used in SI engines adapted for ethanol in so called flexible-fuel vehicles (FFVs). The new models of light vehicles running on E85 are being introduced to the European market. E85 fuel is commercially available in the USA, France, Sweden, and a few other European countries, since the infrastructure for production, delivery and sale of E85 is already developed there. In Sweden, the whole 65% of all gas stations offer E85 [4], while this number is lower in the USA at around 7% [5][6]. Nearly 8.3% of light vehicles in year 2019 were FFV in the USA [7][8]. Approximately 1% of all cars registered in Sweden since 2010 can be run on E85 [9]. This notable difference is due to the fact that FFVs are considered as alternative fuel vehicles (AFVs) in the USA [10]. With the uncertainty that EU tax exemption measure for biofuels expiring at the end of year 2022 creates, E85 is not a favourable fuel in Sweden currently, despite its availability [11].

A report by Swedish Energy Agency [12] which includes a well-to-wheel analysis of different liquid fuels and electricity, shows that GHG emissions per energy content during the whole lifecycle of the fuel are reduced by 45% when E85 is used compared to gasoline, and 36% compared to diesel. The ethanol used for E85 in Sweden is 81% of fossil-free origin. First-generation (1G) ethanol is traditionally made through biological processes, such as fermentation of biomass, usually from sugarcane, sugar beets, grains or corn. New production processes, including pre-treatment, enzymatic hydrolysis and fermentation, that reuse waste products from other industries, such as lignocellulose residues (pulp and paper), have been developed. Since this kind of renewable and sustainable ethanol fuel production does not compete with food industry for the natural resources, the product is called second-generation (2G) ethanol. In integrated bio-refineries, the total lignocellulosic biomass is valorised by producing valuable speciality chemicals alongside 2G ethanol. The energy platforms for burning lignocellulose residues in boilers for co-generation of heat and power (CHP) are already well-established and can be used in 2G ethanol production as well [13]. Further potential of E85 fuel lies in the possibility to additionally reduce the GHG emissions by exchanging a portion of gasoline with biogasoline, i.e. renewable gasoline that is a side product of making renewable diesel [14] or bio-based gasoline, made of residuals from the forest industry, hemicellulose and cellulose based sugars.

A combustion concept that can derive benefits from properties of ethanol and gasoline combustion in a DICI engine is partially premixed combustion (PPC), which can be classified as low temperature combustion (LTC) [15]. Fuel injected during the last quarter of the compression stroke creates sufficient premixing, avoiding fully premixed or fully heterogeneous conditions, and the auto-ignition occurs after a delay. The reduced fuel-air equivalence ratio and compression temperature lower than in conventional diesel combustion (CDC) enables avoiding the formation of soot and NOx simultaneously [16]. This is possible to achieve by boosting the intake air pressure and diluting the mixture with an excess of air, or by using EGR or water injection to add new gas ingredients and increase the heat capacity of the mixture [17][18][19]. Fuels appropriate for PPC have high enough autoignition resistance, i.e. high RON ratings [20][21][22].

Alcohol blends can be used in different ways in the ICEs, as summarised in [23]. The benefits of using low-sooting ethanol fuels in DICI engines were initially presented in [24]. E85 combines the properties of the two high RON fuels: ethanol [25] and gasoline [26], making it a good candidate for a DICI fuel [27][28]. Literature on using E85 in heavy-duty (HD) or DICI engines is scarce, since E85 is a fuel traditionally used in low-duty direct ignition spark ignited (LD DISI) engines [31][30] and more recently in a concept powertrain in medium-duty (MD) DISI trucks [31]. The observed benefits of lower soot levels, GHG, and other engine out emissions from DISI engines initiates the idea of testing E85 in DICI engines.

ED95 is a fuel commercially used in HD CI engines [32][33]. It consists of 95% hydrous ethanol by volume, 5% by weight are ignition improver polyethylene glycol derivatives, and 2.8% by weight is corrosion inhibitor methyl tert-butyl ether and isobutyl alcohol. Since the ethanol in ED95 is hydrous, the fuel contains 6.4% water by weight. An ED95 engine is similar to a diesel engine with modified fuel system and considerably higher compression ratio (r_c) of 28:1, making the engine bigger and more complex and its operation costly. Another drawback is that ED95 fuel is not readily available and that the technology is developed by only one engine manufacturer. The reported benefits are significantly reduced THC, CO and NOx tailpipe emissions, despite the aftertreatment systems not being optimized for the operating conditions [34].

The reactivity-controlled compression ignition (RCCI), being another LTC concept, uses a port fuel injected (PFI) low reactivity fuel, with direct injection (DI) of a smaller amount of a high reactivity diesel fuel. Several studies were conducted on E85 in combination with diesel fuel as ignition improver in dual fuel LD [35] and HD [36][37] CI engines. RCCI is, however, limited by the complexity of the fuel storage and supply system. A study with only E85 in a HD CI engine is presented in [38], where PFI and DI were utilized simultaneously.

Heavy-duty engines operating over low load duty cycles are typical for urban environments and vocational applications, such as delivery trucks and refuse pickup. Urban areas require large quantities of goods and services for commercial and domestic use. During the COVID-19 pandemic, only food delivery has more than doubled in the USA [39]. Around 90% of population in Europe is shopping online and has their orders delivered [40]. Therefore, the relevance of low load engine emissions is increasing beyond the emission regulations in force. Currently, 45% of HD engine tests in World Harmonized Stationary Cycle (WHSC) are performed at low load, i.e. at 25% of the full engine load [41].

This study aims to fill the knowledge gap about DICI of E85 in a HD engine. Three parameters controlling the combustion processes in the engine are varied within a certain range in a Box-Behnken design (BBD) of experiment which gives 13 engine operation points in LTC combustion mode at mid-to-low load. The focus lies on identifying conditions for a high gross indicated efficiency (GIE) and low indicated specific (IS) gaseous emissions and soot levels. These emission levels are compared to the EURO VI emission standards for HD vehicles which is introduced in Europe in 2014 [42].

Method

Experimental Setup

Experiments were performed on a test rig based on a Scania D13 six-cylinder HD DICI engine. Figure 1 shows the schematic diagram of the experimental engine and surrounding setup. One of the cylinders was active and the fuel was injected through an injector with 12 holes of 230 µm diameter and 120° umbrella angle connected to a common rail and a high-pressure injection (XPI) fuel pump. The fuel supply system on this engine was designed for a Scania ED95 ethanol engine suited for operation with alcohols. The existing equipment was used and therefore the engine piston was of the standard stepped bowl shape with geometrical r_c of 17.3:1. Table 1 lists the specifications of the experimental engine.

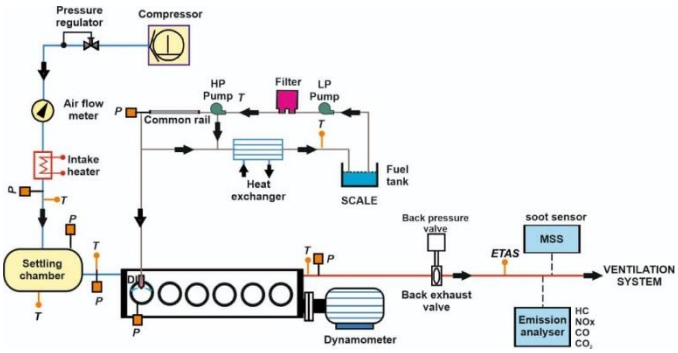

Figure 1. Schematic diagram of the experimental engine. Reprinted from [43] with permission.

Table 1. Specifications of the experimental engine

Cylinders	originally six, operated on one (cylinder 6)
Displacement volume	2124 [cm^3]
Stroke	160 [mm]
Bore	130 [mm]
Connecting rod length	255 [mm]
Geometrical r_c	17.3:1
Number of valves	4

An external compressor provided the oil-free dry air for the engine. In order to achieve a stable intake charge temperature, a 7.5 kW heater was placed in the intake pipe. The engine was connected to an electric motor that motored the engine during the start-up phase, and kept the engine at a constant rotational speed when fired. A water cooled Kistler pressure transducer measured the relative in-cylinder pressure. The cylinder pressure at the inlet bottom dead center (BDC) was considered equal to the intake manifold pressure when the absolute in-cylinder pressure was calculated for the heat release calculations. Also, the top dead center (TDC) offset between the CAD measured by the encoder signal and the calculated in-cylinder volume was compensated for by setting the peak of the motored in-cylinder pressure at a fixed location, as explained in [44].

The value of lambda (λ) was measured in real time by an ETAS LA4 meter. An AVL micro-soot sensor (MSS) was used to continuously

measure the equivalent black carbon (eBC) mass concentration of soot in the engine-out exhaust stream [45][46]. A Horiba emission system (MEXA-7500DEGR) analysed the gaseous emission levels in the raw exhaust without using aftertreatment systems: THC, CO, NOx and O_2. A flame ionization detector (FID) in the emission analyser was not optimal for measurement of exhaust from partially oxidized fuels, such as E85, since it underestimated the THC concentration. According to studies [47][48], the realistic THC values may be higher by 15–18% than the ones measured by FID. However, the suggested correction factors were not included in the results presented in this publication.

The E85 fuel used throughout this study was a commercially available summer blend of 85 volume-% of bioethanol and 15 volume-% of gasoline with properties shown in Table 2. In order to increase the lubricity of E85 and ensure flawless operation of the fuel delivery system, 200 ppm of Infineum R655 was added to the E85, and its effect on the results was considered negligible [49].

Table 2. E85 fuel specifications. *Provided by the manufacturer [50], other values from [51].

RON	101–104*
H/C	2.703
O/C	0.382
Q_{LHF}	29.62 MJ/kg
$(A/F)_S$	9.85

Experimental Design

Since the response of an experiment can be affected by numerous factors, this experiment was limited to manipulating three chosen factors. A BBD with 13 operation points (OPs) limits the test points compared to a full factorial (27 points), and at the same time avoids extreme combinations of control values that could be obtained by a 15 points central composite design (CCD) [52].

A BBD was applied in this experiment in order to, with a limited number of measurement points, collect the data that can characterise a wide field of DICI operation with E85. The most important engine control parameters were used as design factors in order to catch and describe their effects on the engine performance, as well as to determine interactions between them which otherwise might not be possible to see. These control parameters are the fuel injection pressure (P_{rail}), air-fuel ratio expressed as λ, and combustion phasing measured after top dead centre (ATDC) as the crank angle at which 50% of the charge has been consumed (CA50). Each of them has three levels coded as -1, 0 and 1, responding to a low, middle and high level setting, respectively, as shown in Table 3. The BBD points are visually represented in Figure 2, and specified in Table A-1 in Appendix. The physical values of the factor settings were decided during the initial tests of the engine operation limits at a constant load of 8 bar gross indicated mean effective pressure (IMEP). A signal sent to the fuel injector directly controls P_{rail}, and fine-tuning the start of injection (SOI) sets CA50 to a desired value. The value of λ is changed by adjusting the intake air throttle. Note that the middle level of λ was not possible to set to a mean between high and low level values due to the limitations in hardware controllability. The closet achievable value was chosen. Operational values of CA50 and λ were positioned with maximum ±0.27 CAD (2.85%) and ±0.1 (5.35%) of the nominal values, respectively.

The in-cylinder pressure data used in this study were collected from the engine by sampling signals every 0.2 CAD and averaged from 300 engine cycles measured under steady state engine operation conditions at the constant rotational speed of 1200 rpm, constant intake temperature (T_{in}) of 120°C and constant gross IMEP of 8 bar. The exhaust gas recirculation (EGR) valve was sealed to prevent any leakage and ensure there was no EGR.

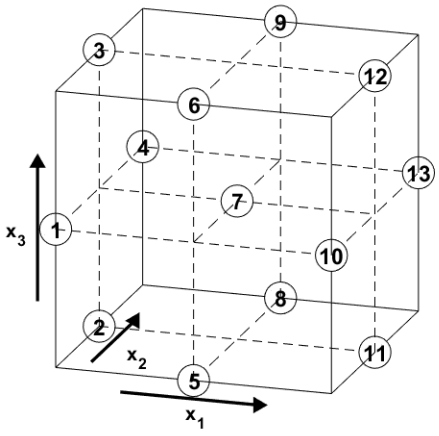

Figure 2. Engine operation points in a Box-Behnken design with three factors x_1, x_2 and x_3

Table 3. Coded and physical values of the BBD factors

Coded units	P_{rail} [bar] (x_1)	λ (x_2)	CA50 [CAD ATDC] (x_3)
-1	800	1.25	6
0	1050	2.3	8
1	1200	3	10

Regression Model

In order to mathematically describe and study the effects of the engine control parameters on the engine behaviour, five multiple linear regression (LR) models of engine GIE, IS THC, CO, NOx and soot were built. The purpose of the presented models is to provide a better understanding of the processes behind the engine behaviour with E85 fuel, and not to provide a predictive tool for an engine efficiency and emissions.

The predicted response Y is represented in Equation 1 as a linear combination of calculated regressors β with three predictors x_1, x_2 and x_3 which correspond to P_{rail} [bar], λ and CA50 [CAD ATDC], respectively. Calculations are performed with the normalized coded units (Table 3), and therefore the effect of the physical units on the magnitude of the predictors is removed.

$$Y = \beta_0 + \beta_1 x_1 + \beta_2 x_2 + \beta_3 x_3 + \beta_{12} x_1 x_2 + \beta_{13} x_1 x_3 + \\ + \beta_{23} x_2 x_3 + \beta_{11} x_1^2 + \beta_{22} x_2^2 + \beta_{33} x_3^2 \quad (1)$$

The coefficient of determination R^2 indicates the quality of a model fit to the measured data, where $R^2 = 0$ means no fit at all, and $R^2 = 1$ means a perfect fit. In some cases, it is not possible to obtain great models with high R^2. Introducing variable transformations may improve a model which, for example, predicts a physically impossible negative response. Predictors x_1, x_2 and x_3 are in that case replaced with their logarithmical values $\log x_1$, $\log x_2$ and $\log x_3$, respectively, making a new model, and finally the physical response is computed as 10^Y.

Results

Model Calculation

Table 4 lists the R^2 values showing that models could capture high percentage of the variations in response to the independent engine control parameters. A logarithmic regression model was needed for IS soot due to low measured values. The values of calculated regressors β are listed in Table A-2 of Appendix.

Table 4. Coefficients of determination for the LR models of GIE and IS emissions

	GIE	THC_{is}	CO_{is}	NOx_{is}	$Soot_{is}$ (log)
R^2	0.89	0.97	0.89	0.88	0.98

The modelled influence of the control parameters on the engine performance can be seen in Figure 3. The bars are sorted in declining order and represent the absolute values of the model regressors (the blue ones have positive and grey negative signs) with the standard error of the mean (SEM) lines. A higher magnitude of a regressor shows a stronger influence of the control parameter on the output. Red axis on the right-hand side shows the accumulated sum of the influence of each consecutive control parameter. Apart from showing which control parameters are important in controlling the engine behaviour, the models also reveal which control variables do not affect the measured outputs.

There is a fairly good correlation between experimental and modelled results for GIE, with R^2 at 0.89. Figure 3 shows that the GIE is mainly influenced by λ and an interaction between P_{rail} and λ. The SEM of P_{rail} regressor is considerably higher than the magnitude, therefore a direct influence of P_{rail} on of GIE cannot be confirmed. Of these three factors, IS THC emissions depend on λ and λ^2, as well as P_{rail}, and R^2 of this model is high at 0.97. IS CO model, with R^2 of 0.89, in a similar manner includes the strongest influence of λ and λ^2. As in the case of GIE, the effect of P_{rail} on IS CO is not conclusive, but still visible in the interaction between P_{rail} and λ. The logarithmic IS soot model is reliable with R^2 at 0.98, with all three control parameters having a considerable influence on the output. Similarly, the IS NOx emission model shows that all predictors affect the output. The effect of CA50 is not statistically significant, however it is included through its squared term. A logarithmic variable transformation would not increase R^2 of the IS NOx model, so the original model with R^2 of 0.88 was studied.

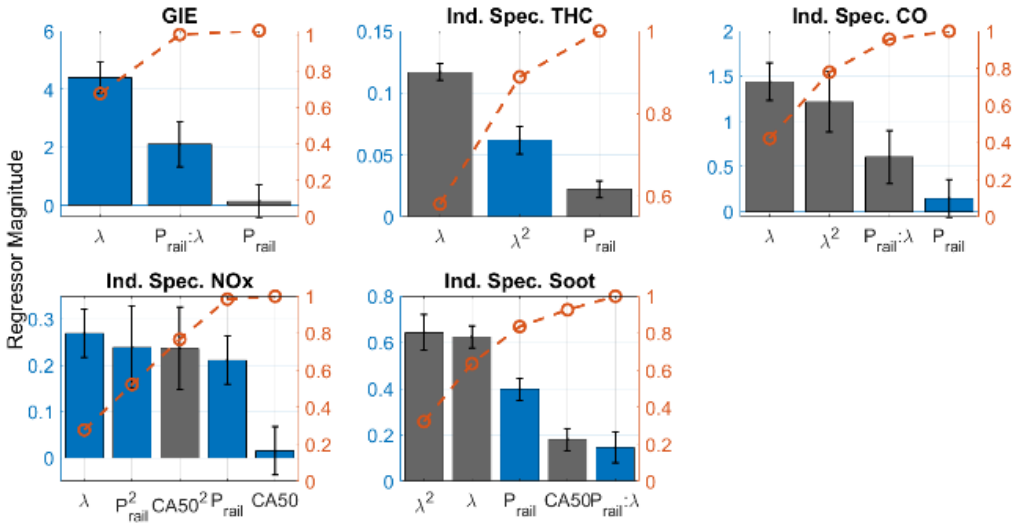

Figure 3. Ranking of the absolute values of control parameters by their influence on GIE, IS THC, IS CO, IS NOx, and IS soot

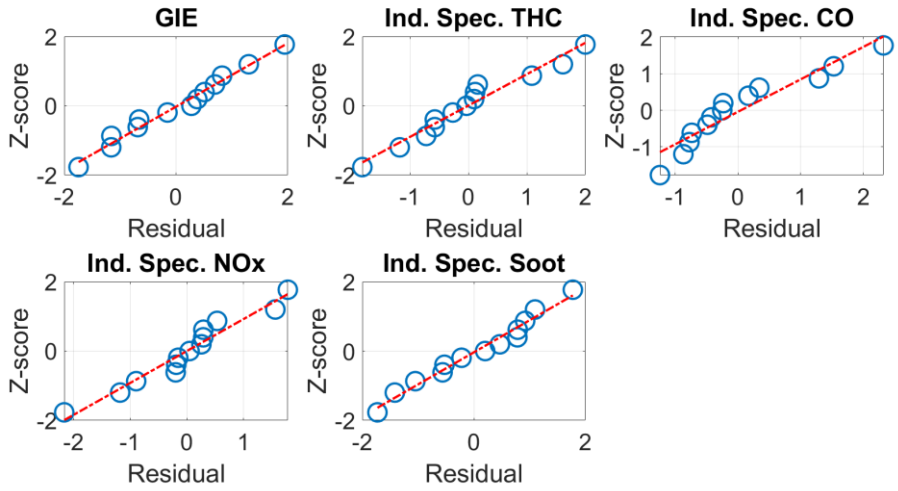

Figure 4. Normal plot of residuals for the LR models of GIE, IS emissions and soot

The normality of residuals from the obtained regression models is validated by plotting them against Z-score. Figure 4 shows that the points have fairly symmetric distribution around a straight line of a normal plot with no major outliers for all five modelled responses, which indicates that the normality assumption of the measurements is satisfied.

Engine Performance and Emissions

Two examples of the rate of heat release (RoHR), in-cylinder pressure and injector current within a relevant window of crank angles for OP4 (P_{rail} at the low setting, λ at the high setting, and CA50 at the medium value) and OP7 (the central BBD point) are shown in Figure 5. The injector current represented by a black line is only an indication of the actual SOI and end of injection (EOI). The EOI is clearly separated from the start of combustion defined as CA5, which gives a positive mixing period (MP). For all 13 OPs, the MP is positive in the range from 2.8 to 5.1 CAD, indicating that the combustion mode is LTC, PPC in particular [53], with very short combustion durations (11–22 CAD), which is one of the factors contributing to high efficiency (see Figure 7a). Throughout the experiments, the combustion was stable with the coefficients of variation (COV) of net IMEP in the range between 1.7 and 2.8%.

The predicted model responses for the efficiency and emissions are compared to the measured values and presented in the two following sections. The trends of emissions are also discussed in comparison with typical emission levels with diesel fuel available in literature and with respect to the stationary EURO VI emission standards for HD vehicles given in Table A-3 in Appendix.

The dashed lines in Figures 8, 9, 10, 12 and 13 are model outputs for the coded value –1 of a control parameter in the corresponding legend (low level). Likewise, the solid lines represent model outputs for the coded value +1 of a control parameter in the legend (high level). In both cases, the other control parameter (not present in the legend) is set to the middle level (coded as 0). Experimental measurements in the graphs are represented as o for a low control parameter setting and x for a high setting.

Efficiency

The majority of OPs lies in a GIE range right below 45%, see Figure 7a. The four OPs with lowest GIE (OPs: 1, 5, 6 and 10) are the cases with λ at 1.25, having the highest maximum average in-cylinder temperature (see Figure 7c) resulting in higher heat losses, but low THC emissions due to high temperatures, see Figure 6. Higher CO emissions (also in Figure 6) result in their combustion efficiency (η_c), shown in Figure 7b, being slightly lower than of the other OPs. This implies that THC and CO emission behaviour depends strongly on λ (confirmed by models in the following two subsections); with λ of 1.25, a dependency close to linear between THC and CO has a steeper slope, whereas the dependency slope is less steep for the other two λ values (2.3 and 3).

Despite its η_c being close to the aforementioned group of OPs, OP4, with P_{rail} at the low setting, λ at the high setting, and CA50 at the medium value, has the highest achieved GIE of 50.23%. OP4 has, though, emissions completely opposite to the previous OPs group, with high THC and low CO emission levels.

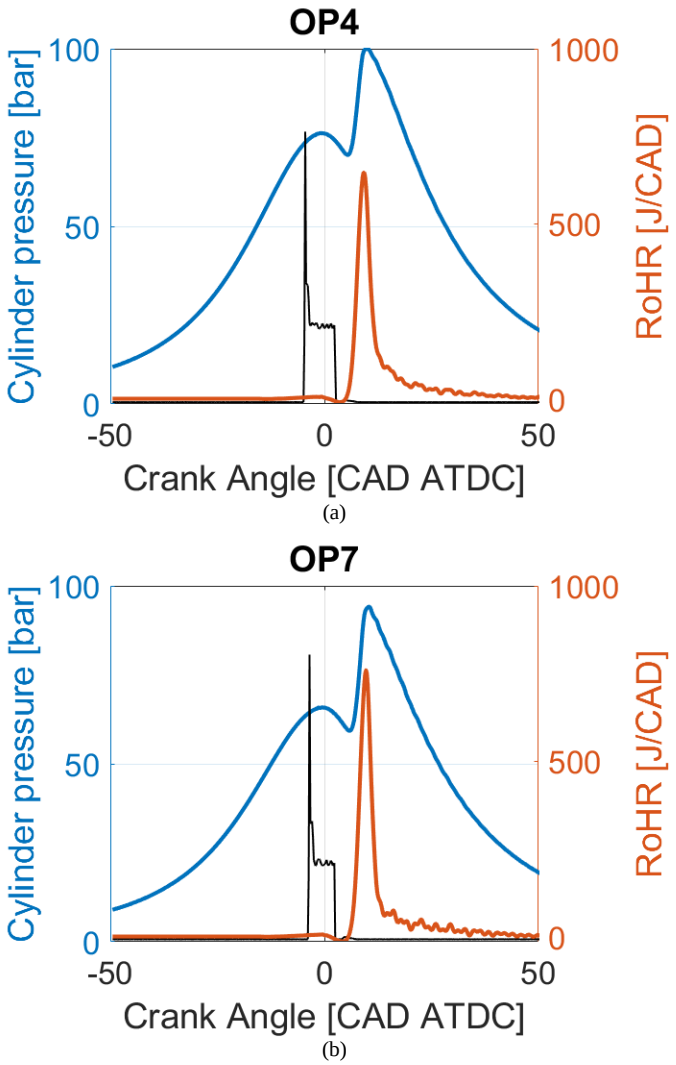

Figure 5. RoHR, in-cylinder pressure, and injector current for OP4 (a) and OP7 (b). For OP nomenclature see Table A-1 in Appendix.

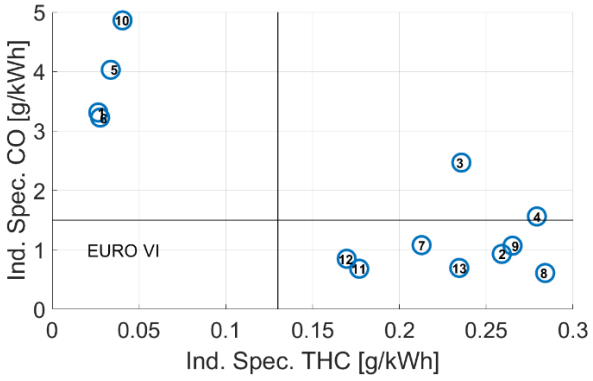

Figure 6. IS CO versus IS THC for the 13 OPs, and EURO VI emission standard limits. For OP nomenclature see Table A-1 in Appendix.

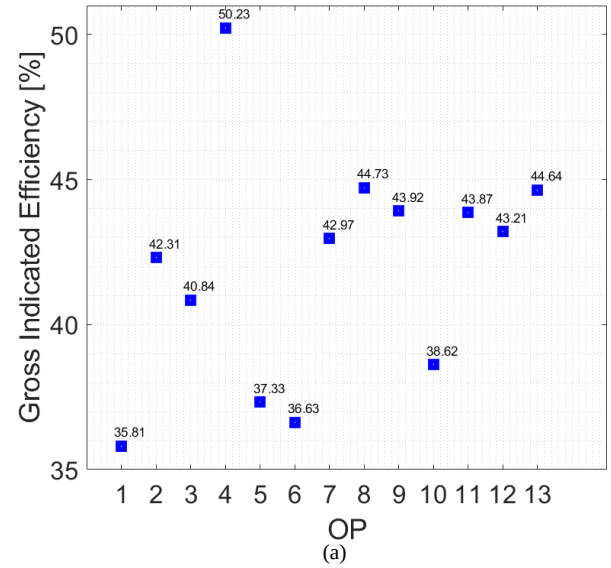

(a)

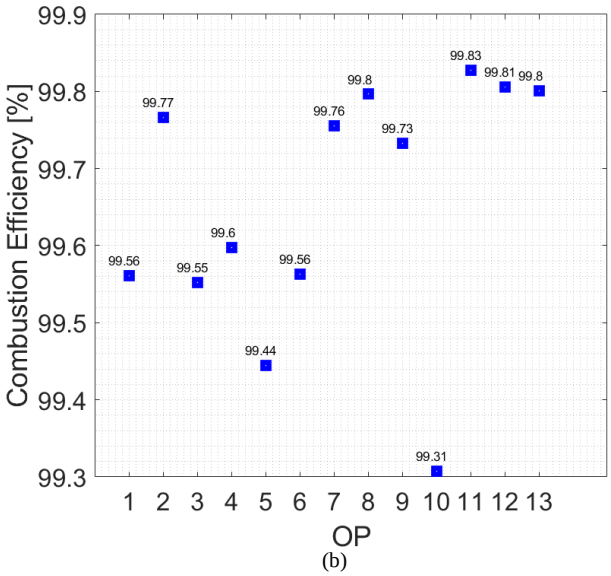

(b)

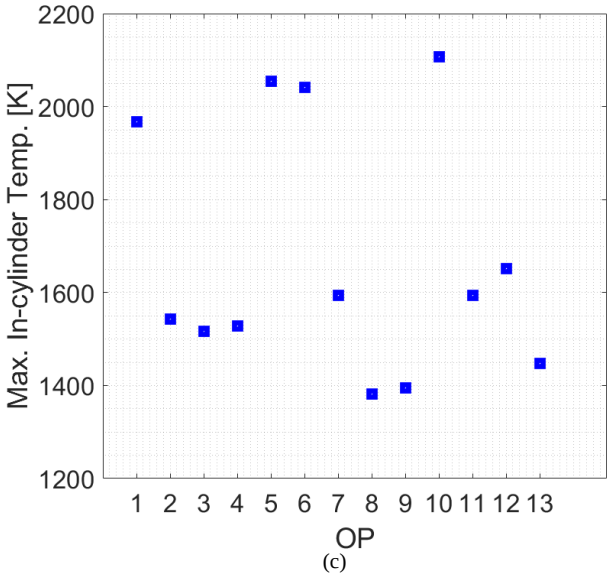

(c)

Figure 7. GIE (a) and η_c (b) and maximum in-cylinder temperature (c) for the 13 OPs. For OP nomenclature see Table A-1 in Appendix.

OP4 is a candidate for the most favourable operation condition within the range tested in this experimental study. The reason for the high GIE may be that λ at 3 is better for thermodynamic efficiency, and that CA50 at the middle setting (8 CAD ATDC) is nearest to the optimal. The maximal in-cylinder temperature of OP4 is similar to those of OP2 and OP3, and it is reached at similar CAD, but the average in-cylinder temperature drops faster for OP4 due to its shorter burn duration than for OP2 and OP3. Lower P_{rail} of 800 bar in combination with the previously mentioned settings gives the operation conditions of this engine configuration that can be a starting point for a further investigation, due to a big step up in GIE compared to the other OPs.

The GIE model shown here is able to capture the trends of the experimentally measured physical values. The increase in P_{rail} (see Figure 8b) in richer combustion conditions increases the air entrainment and promotes mixing, which results in higher efficiency, whereas GIE decreases due to the excess air at the highest λ value. It corresponds well to the steeper increase in GIE for lower P_{rail} when λ changes from the low to high setting, as it can be seen in Figure 8a. This may indicate that the local maxima of the efficiency are outside of the range tested here, when GIE values will start decreasing again for even leaner mixtures.

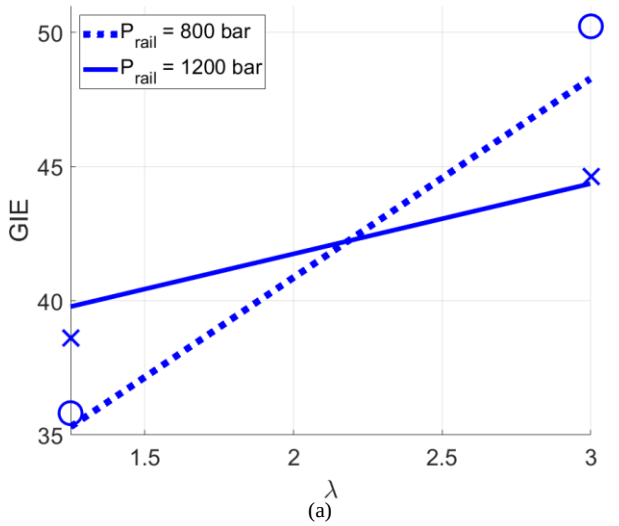

(a)

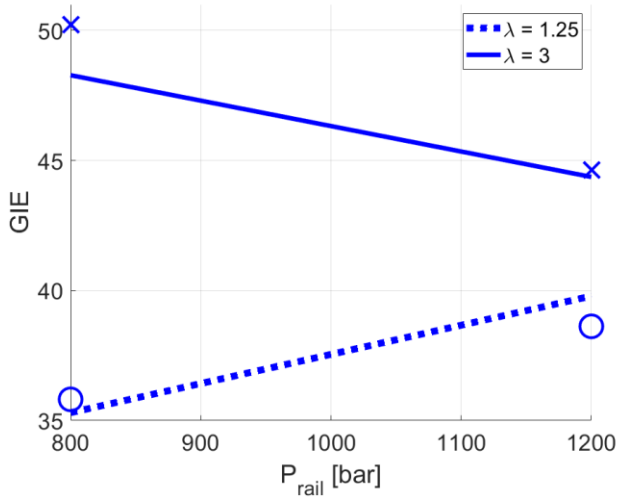

(b)

Figure 8. The effect of the control parameters on GIE, (a) λ, (b) P_{rail}

Indicated Specific THC

The effects of λ and P_{rail} on IS THC are shown in Figure 9. THC emerging during expansion and exhaust strokes is not further oxidized in OPs with higher λ and lower exhaust temperatures. In case where P_{rail} is increased for the low λ setting, the model is not able to predict a slight increase in IS THC emissions, whereas it follows the trends for the leaner mixture.

A previous study (see [46]) with the same experimental setup and operation conditions similar to OP11, showed 25% lower IS THC emissions with diesel fuel compared to E85 in this study. Since the injectors used here were not targeted for E85 fuel, this would be a possible degree of freedom for lowering THC emissions. In general, it is expected that THC emissions will be higher due to higher latent heat of vaporization of ethanol compared to diesel.

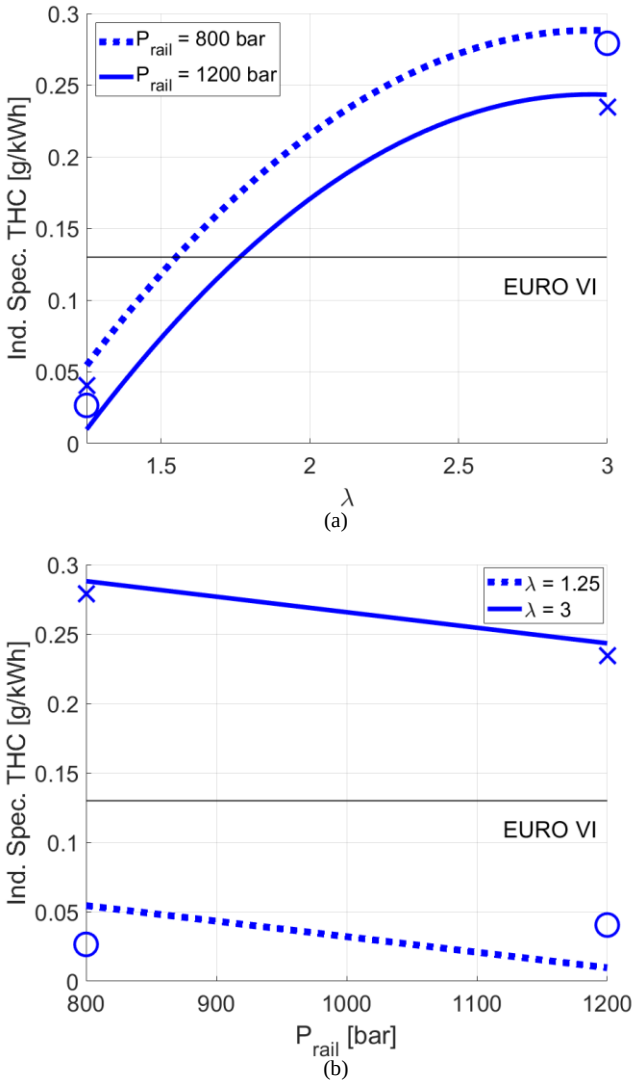

Figure 9. The effect of the control parameters on IS THC, (a) λ, (b) Prail

Indicated Specific CO

IS CO emissions in this study are lower than the EURO VI standard, except for the OPs with low λ settings, see Figure 10. More air available for the combustion provides the conditions for complete oxidation to CO_2. One exception to this is OP3 (see Figure 6) where λ is at the medium level: the IS CO emission is slightly increased, possibly due to the retarded combustion, leaving less time for oxidation after combustion.

The trends of the measured values are captured by this model. However, the modelled output values at the high setting of P_{rail} underestimate IS CO values.

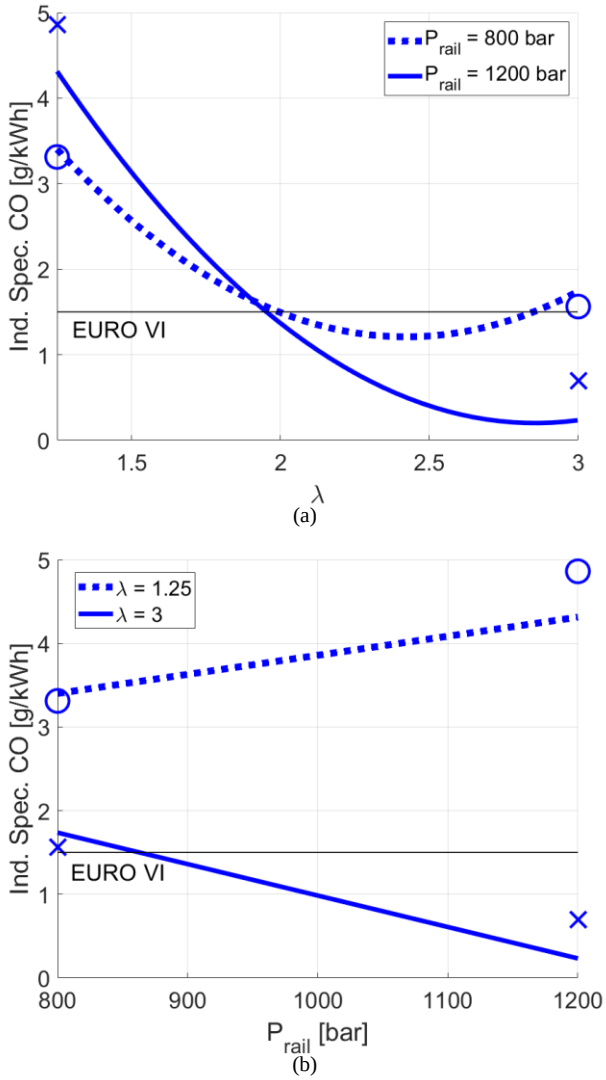

Figure 10. The effect of the control parameters on IS CO, (a) λ, (b) Prail

Indicated Specific NOx

The regression model of IS NOx in Figure 11 includes an almost equally strong influence of all three control variables, describing the NOx trends well; however, it is not able to capture the steeper increase of the emissions for higher levels of P_{rail} as well as for the retarded combustion phasing. The NOx formation rate has an exponential dependency on combustion temperature, as explained in [54]. The LR model in this study includes quadratic terms of P_{rail} and CA50 in an attempt to mimic the non-linearity.

The experimental measurement presented in Figure 12 show that the high λ value, with more oxygen available for the combustion, results in higher NOx emissions. OP 4 is the only exception to this, since the NOx level there is comparable to the OPs with the low λ values. The peak cylinder temperatures with leaner mixtures are considerably lower than for the OPs with lower λ values, as shown in Figure 7c, but still their NOx emissions are high. This difference may be due to higher latent heat of vaporization of ethanol compared to diesel, and its cooling effect which decreases NOx formation when the mixture is richer.

Higher P_{rail} increases the air entrainment and promotes mixing of fuel, causing a faster combustion with shorter burn durations, and therefore higher peak in-cylinder temperatures and higher NOx emissions. Earlier combustion in combination with the P_{rail} increase gives higher increase in NOx emissions than later combustion when P_{rail} increases.

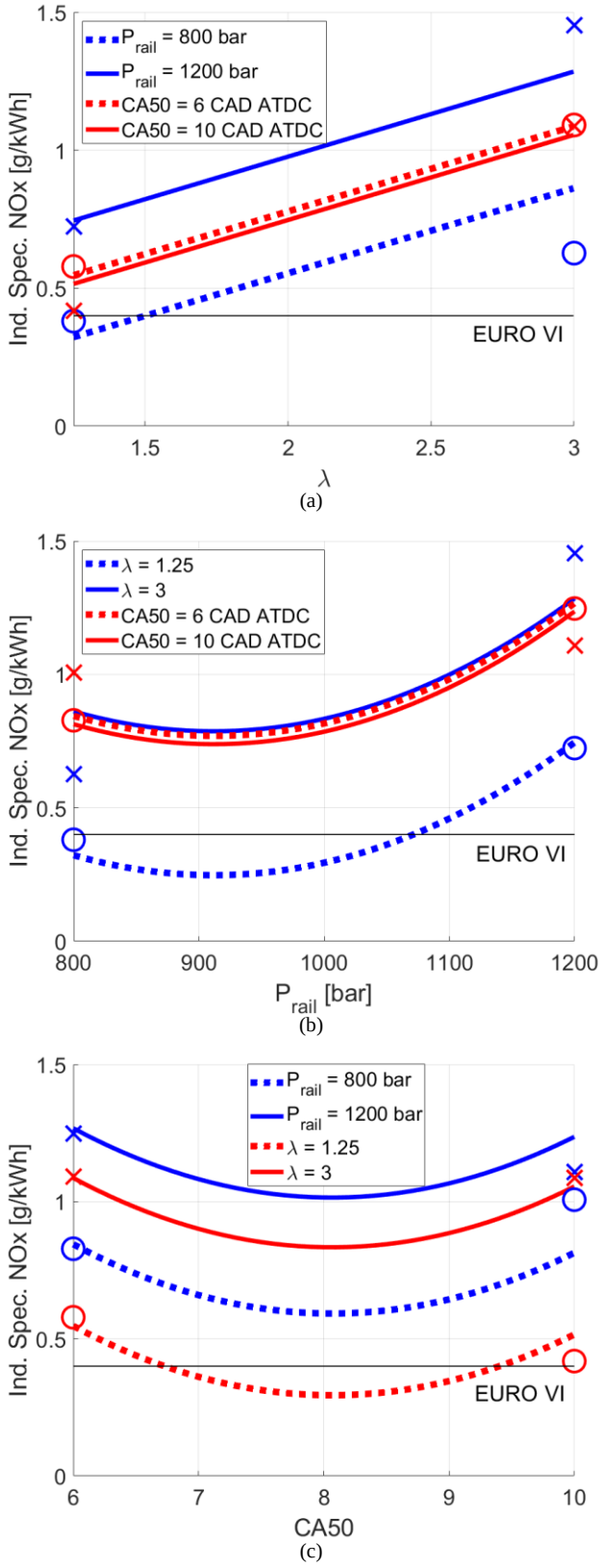

Figure 11. The effect of the control parameters on IS NOx, (a) λ, (b) Prail, (c) CA50

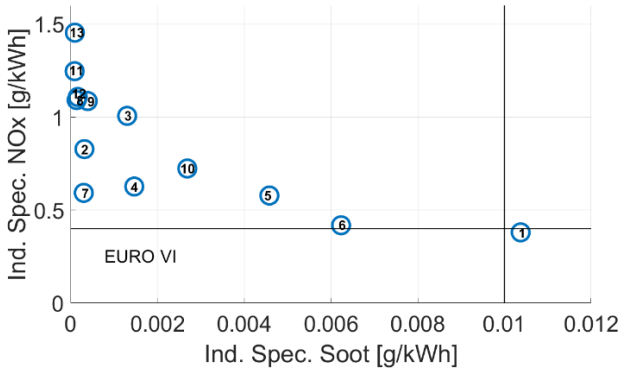

Figure 12. NOx – soot trade-off for the 13 OPs, and EURO VI emission standard limits. For OP nomenclature see Table A-1 in Appendix.

Due to the PPC-type combustion of E85, where most of the combustion takes place in the premixed mode, NOx emissions are significantly lower relative to CDC observed in [46]. Still, the NOx levels are higher than the EURO VI standard, and a reduction would be possible by utilizing EGR [27].

Indicated Specific Soot

A power law model of soot emissions from diesel combustion, where soot depends on CA50, τ (half life of heat release after end of injection), IMEP and intake oxygen concentration, was previously described in [55]. The last two variables are constant in this study, whereas the first two are changing: CA50 and τ (CADs needed for the RoHR to diminish by half from the peak, indicating the efficiency of the late cycle oxidation). Despite the soot formation and oxidation processes being non-linear, there is a possibility to represent the engine-out soot emissions by a LR model, which in this study includes λ, showing the availability of oxygen and directly affecting the rate of soot oxidation, P_{rail}, indicating the mixing rate, and CA50, a measure of the time available for oxidation before opening of the exhaust port.

The regression model of soot is capturing the measured values well, see Figure 13. A higher P_{rail} promotes mixing rate by better fuel atomization and penetration, avoiding local rich zones, which results in lower soot levels. An advanced CA50 allows for longer time available for soot oxidation, also reducing the soot levels. At the high λ setting, soot emissions are low, since more air is available for the oxidation.

All operation points except for OP1 showed soot levels under the current emission regulations. The models rely on the average IS soot value for all 300 observed engine cycles, however, COVs of the measurements from MSS in three OPs with lowest soot levels are over 20%, even though the sensitivity of MSS is such that it should be able to catch these low soot levels. Therefore, it can be argued that measured soot levels from E85 combustion in this study do not fall under measurement or experimental uncertainty, but that the actual soot levels in certain OPs have high cycle-to-cycle variations. High COV values for cycle-resolved soot measurements are common, as [56] shows it in detail.

For the studied OPs, Figure 12 shows that the NOx–soot trade-off can be better handled in combustion with E85 fuel due to its very low soot values and lower NOx values compared to similar low load conditions with diesel fuel previously studied in [46] and gasoline, methanol and ethanol used with a lower r_c in [57].

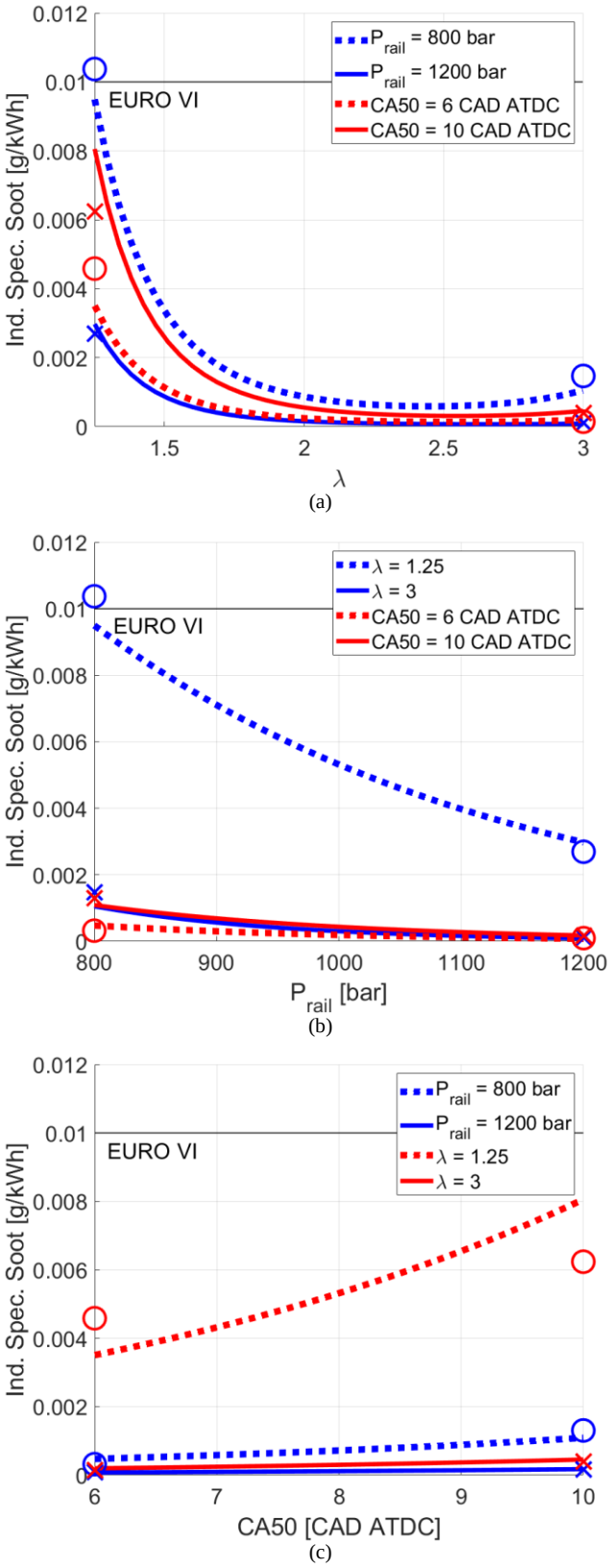

Figure 13. The effect of the control parameters on IS soot, (a) λ, (b) P_{rail}, (c) CA50

Conclusion

Introducing a new fuel and a new engine combustion concept simultaneously in order to combat the climate change can be a challenging and time-consuming task. On the other hand, E85 fuel, being already available on several markets, gives a viable and a relatively fast opportunity to reduce GHG emissions from the HD transport sector. Moreover, it can be used in engines based on the current DICI technology with certain adaptations. The need for high intake air temperature can be removed by by-passing the engine intercooler in order to gain more compression heat [2], or by insulating combustion chamber to reduce heat losses [3]. A difficulty is that a lubricity additive is necessary to protect the high-pressure injection system from ethanol, so an additional tank for that would be needed.

As a part of this study, commercially available E85 was directly injected into a HD CI engine with one active cylinder achieving PPC at mid-to-low load, and the resulting efficiency and emissions were studied.

A BBD of response surface methodology was used to investigate the effects of three control parameters (P_{rail}, λ and CA50) on the E85 combustion. Mathematical models of five experimentally measured and calculated variables (GIE, IS THC, IS CO, IS NOx and IS soot) were then build using linear regression. The simple LR models could describe the behaviour of the engine well, showing that λ and P_{rail} had the influence on the efficiency and all emissions, whereas CA50 affected only NOx and soot.

GIE of the majority of OPs lies right below 45%. The low λ setting is negatively affecting GIE. At P_{rail} of 800 bar, λ of 3 and CA50 of 8 CAD ATDC, GIE reached the highest value of 50.23%. The potential of this OP with high efficiency needs to be further investigated and can be a starting point for future studies.

With E85 fuel, the emitted soot levels were very low, and therefore the NOx–soot trade-off, which is typical for diesel combustion, disappeared. NOx emissions can be further reduced by introducing EGR in future experiments. CO emissions were lower than the EURO VI standard, except for the OPs with low λ settings, and THC emissions were above the emission standard limits, also with the exception of the same group of OPs. This, however, can be solved by an oxidation catalyst [58], with lower conversion efficiencies for LTC and low load, and higher conversion for mid and high loads with higher exhaust gas temperatures.

Since the combustion system was not optimised for E85 fuel, it is likely that the local conditions drive emissions formation. Future CFD studies could suggest a proper spray targeting with an optimized injection strategy, and with injectors and piston bowl shape for ethanol, which would result in more optimal operation conditions and lower emissions.

The next step is to conduct experimental studies in order to describe the behaviour of E85 within a wider engine load range with appropriate EGR levels.

References

1. European Parliament and the Council, “Directive (EU) 2018/2001 of the European Parliament and of the Council of 11 December 2018 on the promotion of the use of energy from renewable sources,” Official Journal of the European Union L 328/82, 2018.
2. Roberts, G., Johnson, B., and Edwards, C., “Prospects for High-Temperature Combustion, Neat Alcohol-Fueled Diesel Engines,” *SAE Int. J. Engines* 7(1):448–457, 2014, https://doi.org/10.4271/2014-01-1194.
3. Blumreiter, J., Johnson, B., Zhou, A., Magnotti, G. et al., “Mixing-Limited Combustion of Alcohol Fuels in a Diesel

Engine," SAE Technical Paper 2019-01-0552, 2019, https://doi.org/10.4271/2019-01-0552.
4. Drivkraft Sverige, "Försäljningsställen med E85 pump," Accessed: January 10, 2022. http://drivkraftsverige.se/statistik/forsaljningsstallen/forsaljningsstallen-med-e85-pump.
5. U.S. Department of Energy, Alternative Fuels Data Center, "Alternative Fueling Station Locator," Accessed: May 18, 2022. https://afdc.energy.gov/stations#/find/nearest?fuel=E85&country=US.
6. NACS, Advancing Convenience & Fuel Retailing, "U.S. Convenience Store Count," Accessed: May 18, 2022. https://www.convenience.org/Research/FactSheets/IndustryStoreCount.
7. U.S. Department of Energy, Alternative Fuels Data Center, "Flexible Fuel Vehicles," Accessed: May 18, 2022. https://afdc.energy.gov/vehicles/flexible_fuel.html.
8. Davis, S., and Boundy, R., "Transportation Energy Data Book: Edition 40," Oak Ridge National Laboratory, Tennessee, 2022.
9. Transportstyrelsen, "Statistik över koldioxidutsläpp," Last modified: February 2, 2021. http://www.transportstyrelsen.se/sv/vagtrafik/statistik/Statistik-over-koldioxidutslapp.
10. "Energy Policy Act of 1992," HR 776, 102nd Congress, Public Law 102-486, https://afdc.energy.gov/files/pdfs/2527.pdf.
11. European Commission, "Prolongation of the tax reductions for pure and high blended liquid biofuels in Sweden," SA.63198 (2021/N), 2021, https://data.europa.eu/doi/10.2763/32423
12. Energimyndigheten, "Drivmedel 2020: Redovisning av rapporterade uppgifter enligt drivmedelslagen, hållbarhetslagen och reduktionsplikten," ER 2021:29, ISBN: 978-91-7993-039-4, 2021.
13. Silveira, M., Vanelli, B., and Chandel, A., "Chapter 6 – Second Generation Ethanol Production: Potential Biomass Feedstock, Biomass Deconstruction, and Chemical Platforms for Process Valorization," Advances in Sugarcane Biorefinery, Elsevier, 2018, 135-152, https://doi.org/10.1016/B978-0-12-804534-3.00006-9.
14. Aakko-Saksa, P., Rantanen-Kolehmainen, L., Koponen, P., Engman, A. et al., "Biogasoline Options - Possibilities for Achieving High Bio-share and Compatibility with Conventional Cars," *SAE Int. J. Fuels Lubr.* 4(2):298–317, 2011, https://doi.org/10.4271/2011-24-0111.
15. Li, C., "Stratification and Combustion in the Transition from HCCI to PPC." PhD thesis, Lund University, 2018. https://lup.lub.lu.se/record/54165f85-8a5c-4050-88ec-6c1c577bd9e3.
16. Akihama, K., Takatori, Y., Inagaki, K., Sasaki, S. et al., "Mechanism of the Smokeless Rich Diesel Combustion by Reducing Temperature," SAE Technical Paper 2001-01-0655, 2001, https://doi.org/10.4271/2001-01-0655.
17. Manente, V., Johansson, B., Tunestal, P., and Cannella, W., "Influence of Inlet Pressure, EGR, Combustion Phasing, Speed and Pilot Ratio on High Load Gasoline Partially Premixed Combustion," SAE Technical Paper 2010-01-1471, 2010, https://doi.org/10.4271/2010-01-1471.
18. Asad, U. and Zheng, M., "Efficacy of EGR and Boost in Single-Injection Enabled Low Temperature Combustion," *SAE Int. J. Engines* 2(1):1085–1097, 2009, https://doi.org/10.4271/2009-01-1126.
19. Bedford, F., Rutland, C., Dittrich, P., Raab, A. et al., "Effects of Direct Water Injection on DI Diesel Engine Combustion," SAE Technical Paper 2000-01-2938, 2000, https://doi.org/10.4271/2000-01-2938.
20. Hildingsson, L., Kalghatgi, G., Tait, N., Johansson, B. et al., "Fuel Octane Effects in the Partially Premixed Combustion Regime in Compression Ignition Engines," SAE Technical Paper 2009-01-2648, 2009, https://doi.org/10.4271/2009-01-2648.
21. Bakker, P., De Abreu Goes, J., Somers, L., and Johansson, B., "Characterization of Low Load PPC Operation using RON70 Fuels," SAE Technical Paper 2014-01-1304, 2014, https://doi.org/10.4271/2014-01-1304.
22. Leermakers, C., Luijten, C., Somers, L., Kalghatgi, G. et al., "Experimental Study of Fuel Composition Impact on PCCI Combustion in a Heavy-Duty Diesel Engine," SAE Technical Paper 2011-01-1351, 2011, https://doi.org/10.4271/2011-01-1351.
23. Tuner, M., "Review and Benchmarking of Alternative Fuels in Conventional and Advanced Engine Concepts with Emphasis on Efficiency, CO_2, and Regulated Emissions," SAE Technical Paper 2016-01-0882, 2016, https://doi:10.4271/2016-01-0882.
24. Hardenberg, H. and Schaefer, A., "The Use of Ethanol as a Fuel for Compression Ignition Engines," SAE Technical Paper 811211, 1981, https://doi.org/10.4271/811211.
25. Kaiadi, M., Johansson, B., Lundgren, M., and Gaynor, J., "Sensitivity Analysis Study on Ethanol Partially Premixed Combustion," *SAE Int. J. Engines* 6(1):120–131, 2013, https://doi.org/10.4271/2013-01-0269.
26. Kalghatgi, G., Risberg, P., and Ångström, H., "Partially Pre-Mixed Auto-Ignition of Gasoline to Attain Low Smoke and Low NOx at High Load in a Compression Ignition Engine and Comparison with a Diesel Fuel," SAE Technical Paper 2007-01-0006, 2007, https://doi.org/10.4271/2007-01-0006.
27. Manente, V., Johansson, B., and Tunestal, P., "Characterisation of partially premixed combustion with ethanol: EGR sweeps, low and maximum loads", Proceedings of the ASME Internal Combustion Engine Division 2009 Technical Conference, ICES2009-76165, United States, May 3–6, 2009, https://doi.org/10.1115/ICES2009-76165.
28. Manente, V., Johansson, B., and Tunestal, P., "Partially Premixed Combustion at High Load using Gasoline and Ethanol, a Comparison with Diesel," SAE Technical Paper 2009-01-0944, 2009, https://doi.org/10.4271/2009-01-0944.
29. Turner, D., Xu, H., Cracknell, R. F., Natarajan, V. et al., "Combustion performance of bio-ethanol at various blend ratios in a gasoline direct injection engine," *Fuel* 90(5):1999–2006, 2011, https://doi.org/10.1016/j.fuel.2010.12.025.
30. Timonen, H., Karjalainen, P., Saukko, E., Saarikoski, S. et al., "Influence of fuel ethanol content on primary emissions and secondary aerosol formation potential for a modern flex-fuel gasoline vehicle," *Atmos. Chem. Phys.* 17(8), 2017, https://doi.org/10.5194/acp-17-5311-2017.
31. Perfetto, A., Kameshwaran, K., Geckler, S. C., Zope, R. et al., "Ethanol Optimized Powertrain for Medium Duty Trucks," Proceedings of the ASME 2014 Internal Combustion Engine Division Fall Technical Conference, V001T03A014, United States, October 19–22, 2014, https://doi.org/10.1115/ICEF2014-5601.
32. Saccullo, M., Benham, T., Denbratt, I., and Johansson, B., "CI Methanol and Ethanol combustion using ignition improver," SAE Technical Paper 2019-01-2232, 2019, https://doi.org/10.4271/2019-01-2232.
33. Barbosa, F., "Heavy Duty Ethanol Engines - A Sustainable Approach for Transit Bus Fleets," SAE Technical Paper 2015-36-0223, 2015, https://doi.org/10.4271/2015-36-0223.
34. Haupt, D., Nord, K., Tingvall, B., Ahlvik, P. et al., "Investigating the Potential to Obtain Low Emissions From a Diesel Engine Running on Ethanol and Equipped With EGR, Catalyst and DPF," SAE Technical Paper 2004-01-1884, 2004, https://doi.org/10.4271/2004-01-1884.
35. Curran, S., Hanson, R., and Wagner, R., "Effect of E85 on RCCI Performance and Emissions on a Multi-Cylinder Light-Duty Diesel Engine," SAE Technical Paper 2012-01-0376, 2012, https://doi.org/10.4271/2012-01-0376.
36. Benajes, J., Molina, S., García, A., and Monsalve-Serrano, J., "Effects of low reactivity fuel characteristics and blending ratio on low load RCCI (reactivity controlled compression ignition)

performance and emissions in a heavy-duty diesel engine," *Energy* 90(2):1261–1271, 2014, https://doi.org/10.1016/j.energy.2015.06.088.
37. Splitter, D., Hanson, R., Kokjohn, S., and Reitz, R., "Reactivity Controlled Compression Ignition (RCCI) Heavy-Duty Engine Operation at Mid-and High-Loads with Conventional and Alternative Fuels," SAE Technical Paper 2011-01-0363, 2011, https://doi.org/10.4271/2011-01-0363.
38. Wang, B., Pamminger, M., and Wallner, T., "Optimizing Thermal Efficiency of a Multi-Cylinder Heavy Duty Engine with E85 Gasoline Compression Ignition," SAE Technical Paper 2019-01-0557, 2019, https://doi.org/10.4271/2019-01-0557.
39. Ahuja, K., Chandra, V., Lord, V., and Peens, C., "Ordering in: The rapid evolution of food delivery," *McKinsey Insights*, September 22, 2021.
40. PostNord, "E-commerce in Europe," Accessed: February 8, 2022. https://www.postnord.se/siteassets/pdf/rapporter/e-commerce-in-europe-2021.pdf.
41. European Commission, "Commission Regulation (EU) No. 582/2011 of 25 May 2011 Implementing and Amending Regulation (EC) No. 595/2009 of the European Parliament and of the Council with Respect to Emissions from Heavy-Duty Vehicles (Euro VI) and Amending Annexes I and III to Directive 2007/46/EC of the European Parliament and of the Council," *Off. J. of the Eur. Union* L 167/1, 2011.
42. UNECE, "Global technical regulation (GTR) No. 4 – Test procedure for compression-ignition (C.I.) engines and positive-ignition (P.I.) engines fuelled with natural gas (NG) or liquefied petroleum gas (LPG) with regard to the emission of pollutants (ECE/TRANS/180/Add.4)," Geneva, Switzerland, 2007.
43. Bin Aziz, A., "High Octane Number Fuels in Advanced Combustion Modes for Sustainable Transportation." PhD thesis, Lund University, 2020. https://lup.lub.lu.se/record/36d51b09-d87b-43d5-b7a2-5abf30495ac6.
44. Tunestål, P., "TDC Offset Estimation from Motored Cylinder Pressure Data based on Heat Release Shaping," *Oil Gas Sci. Technol. – Rev. IFP Energies nouvelles* 66(4): 705–716, 2011, https://doi.org/10.2516/ogst/2011144.
45. Schindler, W., Haisch, C., Beck, H., Niessner, R. et al., "A Photoacoustic Sensor System for Time Resolved Quantification of Diesel Soot Emissions," SAE Technical Paper 2004-01-0968, 2004, https://doi.org/10.4271/2004-01-0968.
46. Novakovic, M., Shamun, S., Malmborg, V., Kling, K. et al., "Regulated Emissions and Detailed Particle Characterisation for Diesel and RME Biodiesel Fuel Combustion with Varying EGR in a Heavy-Duty Engine," SAE Technical Paper 2019-01-2291, 2019, https://doi.org/10.4271/2019-01-2291.
47. Kar, K. and Cheng, W., "Speciated Engine-Out Organic Gas Emissions from a PFI-SI Engine Operating on Ethanol/Gasoline Mixtures," *SAE Int. J. Fuels Lubr.* 2(2):91–101, 2010, https://doi.org/10.4271/2009-01-2673.
48. Wallner, T, "Correlation Between Speciated Hydrocarbon Emissions and Flame Ionization Detector Response for Gasoline/Alcohol Blends," ASME *J. Eng. Gas Turbines Power* 133(8), 2011, https://doi.org/10.1115/1.4002893.
49. Solaka, H., Tuner, M., Johansson, B., and Cannella, W., "Gasoline Surrogate Fuels for Partially Premixed Combustion, of Toluene Ethanol Reference Fuels," SAE Technical Paper 2013-01-2540, 2013, https://doi.org/10.4271/2013-01-2540.
50. Preem. "Etanol E85," May 23, 2019. https://www.preem.se/contentassets/f9e00fc8bae94eaeaf99c137a1270ac6/etanol-e85.pdf.
51. Kale, V., Santoso, H., Marriott, C., Worm, J. et al., "Combustion Robustness Characterization of Gasoline and E85 for Startability in a Direct Injection Spark-Ignition Engine," SAE Technical Paper 2012-01-1073, 2012, https://doi.org/10.4271/2012-01-1073.
52. Andersson, Ö., "Experiment! : planning, implementing, and interpreting," John Wiley & Sons, UK, 2012, ISBN: 978-0-470-68825-0.
53. Manente, V., Johansson, B., and Cannella, W., "Gasoline partially premixed combustion, the future of internal combustion engines?" *Internat. J. Engine Res.* 12(3):194–208, 2011, https://doi.org/10.1177/1468087411402441.
54. Heywood, J., "Internal Combustion Engine Fundamentals, 2nd edition," McGraw-Hill, New York, 2018, ISBN: 9781260116106.
55. Lequien, G., Andersson, Ö., Tunestal, P., and Lewander, M., "A Correlation Analysis of the Roles of Soot Formation and Oxidation in a Heavy-Duty Diesel Engine," SAE Technical Paper 2013-01-2535, 2013, https://doi.org/10.4271/2013-01-2535.
56. Kheirkhah, P., Kirchen, P., and Rogak, S., "Measurement of cycle-resolved engine-out soot concentration from a diesel-pilot assisted natural gas direct-injection compression-ignition engine," *Internat. J. Engine Res.* 23(3):380–396, 2022, https://doi:10.1177/1468087420986263.
57. Shamun, S., Shen, M., Johansson, B., Tuner, M. et al., "Exhaust PM Emissions Analysis of Alcohol Fueled Heavy-Duty Engine Utilizing PPC," *SAE Int. J. Engines* 9(4):2142–2152, 2016, https://doi.org/10.4271/2016-01-2288.
58. Johnson, T., "Vehicular Emissions in Review," *SAE Int. J. Engines* 9(2):1258-1275, 2016, https://doi.org/10.4271/2016-01-0919.

Contact Information

Maja Novakovic
Division of combustion engines, Energy Sciences
Lund University, Sweden
Maja.Novakovic@energy.lth.se

Acknowledgments

This research was conducted within the KCFP Engine Research Center, supported by the Swedish Energy Agency grant number 22485-4.

Definitions/Abbreviations

1G	first-generation
2G	second-generation
AFV	alternative fuel vehicle
ATDC	after top dead centre
BBD	Box-Behnken design
CA5	The crank angle at which 5% of the charge has been consumed, start of combustion.
CA50	The crank angle at which 50% of the charge has been consumed.
CAD	crank angle degrees
CCD	central composite design

CDC	conventional diesel combustion
CFD	computational fluid dynamics
CHP	co-generation of heat and power
CN	cetane number
COV	coefficient of variation, standard deviation divided by the mean
DI	direct injection
DICI	direct injection compression ignition
DISI	direct ignition spark ignited
eBC	equivalent black carbon
EOI	end of injection
FAME	fatty acid methyl ester
FFV	flexible-fuel vehicles
FID	flame ionization detector
GHG	greenhouse gas
GIE	gross indicated efficiency
HD	heavy-duty
HVO	hydrotreated vegetable oil
ICE	internal combustion engine
IMEP	indicated mean effective pressure
IS	indicated specific
LD	low-duty
LR	linear regression
LTC	low temperature combustion
MD	medium-duty
MP	mixing period
MSS	micro soot sensor
NOx	nitrogen oxides
OP	operation point
PFI	port fuel injection
PPC	partially premixed combustion
Q_{LHF}	lower heating value
r_c	geometrical compression ratio
RCCI	reactivity controlled compression ignition
RoHR	rate of heat release
RON	research octane number
SEM	standard error of the mean
SOI	start of injection
THC	total hydrocarbons
WHSC	World Harmonized Stationary Cycle
WHTC	World Harmonized Transient Cycle
XPI	high-pressure injection
η_c	combustion efficiency
λ	lambda, the ratio between the air-fuel ratio and the stoichiometric air-fuel ratio for the given fuel, $\left(\frac{A}{F}\right)/\left(\frac{A}{F}\right)_S$
τ	half life of heat release after end of injection

Appendix

Table A-1. The BBD of the engine operation points

OP	x_1 (P_{rail})	x_2 (λ)	x_3 (CA50)
1	-1	-1	0
2	-1	0	-1
3	-1	0	1
4	-1	1	0
5	0	-1	-1
6	0	-1	1
7	0	0	0
8	0	1	-1
9	0	1	1
10	1	-1	0
11	1	0	-1
12	1	0	1
13	1	1	0

Table A-2. Calculated regressors for the LR models of GIE, IS emissions and soot

Regressors	GIE	THC_{is}	CO_{is}	NOx_{is}	$Soot_{is}$ (log)
β_0	41.93	0.21	1.2	0.56	-3.54
β_1	0.14	-0.02	-0.15	0.21	-0.4
β_2	4.39	0.12	-1.44	0.27	-0.62
β_3	0	0	0	-0.02	0.18
β_{12}	-2.1	0	-0.6	0	-0.15
β_{13}	0	0	0	0	0
β_{23}	0	0	0	0	0
β_{11}	0	0	0	0.24	0
β_{22}	0	-0.06	1.22	0	0.64
β_{33}	0	0	0	0.24	0

Table A-3. European (indicated specific) emissions standard Euro VI for heavy-duty diesel engines in stationary (WHSC) and transient (WHTC) test cycles

	WHSC	WHTC
CO [g/kWh]	1.5	4.0
HC [g/kWh]	0.13	0.16
NOx [g/kWh]	0.4	0.46
NH3 [ppm]	10	10
PM [g/kWh]	0.01	0.01
PN [#/kWh]	8×10^{11}	6×10^{11}